Restoration of interlaced images degraded by variable velocity motion

Yitzhak Yitzhaky
Adrian Stern
Ben-Gurion University of the Negev
Department of Electro-Optics
Engineering
P.O. Box 653
Beer-Sheva 84105
Israel
E-mail: itzik@ee.bgu.ac.il

Abstract. An interlaced composition of odd and even subimage fields is a very common video formation technique. Motion degradation is an inherent problem in portable imaging systems, such as airborne imaging, mobile phones, robots, etc. When relative motion between the interlacing camera and the scene occurs during imaging, two distortion types degrade the image: the edge ''staircase effect'' due to shifted appearances of objects in successive fields, and blur due to scene motion during each field exposure. In contrast to other previous works that dealt with only uniform velocity motion, here we consider a more general, realistic, and complicated case, in which the motion velocity is not necessarily uniform. The motion in each field and the displacement are assumed to be space invariant. Since conventional motion identification techniques used in other works cannot be employed in the case of variable velocity motion, a new method for identification of the motion from each field is used, and different point spread functions are identified for each field. The restored image is achieved by deblurring each field separately, and then realigning the fields. Results of motion identification and image restoration for various motion types are presented and analyzed for simulated and real-degraded images.
[DOI: 10.1117/1.1621406]

Subject terms: motion deinterlacing; motion blur; composite frame; displacement vector estimation; motion optical transfer function; image restoration; blur identification.

Paper 020473 received Oct. 28, 2002; revised manuscript received Apr. 14, 2003; accepted for publication May 23, 2003.

1 Introduction

A scanning process with interlace of the order 2 is common in most video sequence acquisition systems. Interlaced imaging was developed originally to increase the frame (field) rate without enlargement of the required bandwidth of the channel, and is still common today. These imaging systems usually produce their pictures by sequentially superimposing the odd and even fields of each image.

If relative motion between the camera and the object occurs, the interlaced image is degraded by two effects: the typical ''staircase effect''[1] and motion blur.[2] The edge staircase effect (or ''comb effect'') is due to the changes of the object's location during the period between the instants of exposures of two successive fields. The blur results from relative motion between the camera and the scene during the exposure of each field. These phenomena are explained in Sec. 2.

Techniques that considered compensation of the motion effect on interlaced images (sometimes referred as motion-compensated deinterlacing) are designed to convert interlaced images to progressive image format.[3–6] Most of these techniques use several frames to estimate the field displacement caused by the motion and usually ignore motion blur. When the blur effect is ignored, the motion that occurs only between frames can be determined by the motion displacement vector (DV), which is the distance between the locations of the same point in two successive fields. A DV estimate can be used to realign the fields. However, a restoration method is incomplete when it takes into account only the field displacement restoration but ignores the blur caused by motion during the nonzero exposure time. Analysis of motion blur and motion blurred image restoration methods can be found in the literature.[2,7–11]

A recent work for restoration of motion distorted composite frames[12] considered both the staircase and blur effects. The two fields of the interlaced image were realigned using the DV estimated from the interlaced image. Assuming uniform velocity motion during the exposure, and knowing the exposure duration, the blur extent was directly calculated from the DV and used to restore the image from the blur effect (deblurring). The deblurring operation could be carried out, since for a uniform velocity motion, the point spread function (PSF) required for this operation is completely determined by the blur extent and direction. However, in most of the cases a uniform velocity motion during the exposure cannot be assumed.

In this work we propose a restoration technique that is not restricted to uniform velocity motion during exposure. Since the fields are acquired at different points in time, a variable velocity motion forms a different blur effect (PSF) in each of the fields. The motion is also assumed to be space invariant, which means that the blur effect is similar across the field and also the displacement between the fields is spatially similar. Such a situation usually occurs when the relative motion is caused by an angular motion of

the camera. When a uniform velocity motion cannot be assumed, the PSF required for the deblurring operation cannot be calculated from the DV. Therefore, the PSF is estimated here from each field separately, using a new method for estimation of the PSF from motion-blurred images.[13] Each field is then deblurred using its estimated PSF. Given the estimated DV, the deblurred fields are realigned to form the restored image. The field deblurring technique used here[13] is unique because it deals with the general case of variable velocity motion, while other techniques[9,11] usually deal with the simpler case in which the motion PSF can be determined by only one or two parameters.[14]

The effects of motion on interlaced images are explained in Sec. 2. In Sec. 3 the image restoration technique is presented; estimation of the DV that provides the displacement of the fields is presented Sec. 3.1, and the method for estimation of the PSF and the deblurring operation as performed for each field are explained in Secs. 3.2 and 3.3, respectively. Restoration results are presented and analyzed in Sec. 4 for simulated and real-degraded images, and summary and conclusions are presented in Sec. 5.

2 Effects of Motion on Interlaced Images

When relative motion occurs between the camera and an object, the same object is acquired at different points in time because of the delay between the acquisitions of the odd and even fields. Therefore, the same object appears shifted in one field with regard to the other. After superimposing (interlacing) the two fields, edge patterns may form the shape of a comb (the staircase effect) as a result of that shift. The edge displacement caused by this effect is greater when the video frame rate is slower or the average relative motion speed is higher.

The motion blur results from relative motion between the camera and object during the exposure of each field. The pixels in the field are smeared according to the motion velocity during the exposure, causing a blurred (low-pass filtered) version of the field. Since a space invariant blur is assumed (usually as a result of angular camera motion in contrast to motion of objects in the image), the degraded field is modeled as a convolution between the ideal field and the PSF, with added random noise.[8–10] The blur extent depends on the average motion speed during the exposure and the exposure duration.[2]

A heuristic illustration of an interlaced image distorted by variable velocity motion is shown in Fig. 1. Figure 1(a) shows the object locations at the beginnings of the exposure instants of two successive fields. A horizontal motion with the velocity of $v(t)$ is assumed, causing a horizontal displacement of

$$s = \int_0^{t_s} v(t)dt$$

between the fields, where t_s is the time between the field exposures. In Figs. 1(b) and 1(c) the blurred odd and even fields are presented. Since the motion velocity is variable, the instantaneous motion velocity $v(t)$ is different at each field, and therefore the gray-level distributions across the smeared object are different at each field. Since the average motion velocity is also different in each field, the resulting blur extents are different in each field. This appearance is different from the case of uniform velocity motion, where each point in the original image is uniformly distributed in the blurred image. The intensity of the smear caused by the variable velocity motion is inverse proportional to the instantaneous velocity. Figure 1(d) shows the interlaced image formatted by superimposing the two fields. The image is degraded by both the staircase effect and the motion blur.

3 Distortion Estimation and Image Restoration

Restoration of motion-distorted interlaced images requires consideration of both blur and staircase (comb) effects. As presented in the previous section, the image distortion characteristics are the PSF, which characterizes the blur, and the DV, which characterizes the staircase effect. Restoration of the image requires knowledge of these distortion characteristics. However, since these characteristics are not *a priori* known, they should be estimated from the degraded image. Image restoration, in which the degradation characteristics are not *a priori* known, is usually termed *blind restoration*. Such a process is termed *blind deconvolution* when the degraded image is modeled by a convolution between the ideal image and the PSF[9] (as is the case with the fields themselves). Since the PSF is generally a low-pass (blurring) filter, the deconvolution is essentially a deblurring operation.

The image restoration process is therefore composed of two stages: one is identification of the distortion characteristics that are the PSF of the blur in each field, and the DV that characterizes the displacement between the odd and even fields. Each field is then deblurred using its identified PSF, and the displaced fields are realigned using the identified DV.

A scheme of the complete restoration process is presented in Fig. 2. The technique for the PSF estimation is presented in Sec. 3.1. The block-matching approach used for the estimation of the DV is presented in Sec. 3.2. Restoration of the image using the identified distortion characteristics is presented in Sec. 3.3.

3.1 *Estimation of the PSF of the Blur in the Fields*

As a result of the motion, each field is blurred according to the motion during its recording exposure. Because the motion is not assumed to have uniform velocity, the PSFs resulted from the motion, which are required to deblur the fields, cannot be extrapolated from the DV as performed in Ref. 12. Therefore, a new blur estimation method recently developed[13] is implemented. The method is performed in a straightforward manner without iterations and it uses the blurred field only as input information.

The blurring process is assumed to be space invariant. The meaning is that the motion does not change according to the location in the image plane. The blurred field is modeled as a convolution between the PSF and the original unblurred field, and the noise is assumed to be additive. This model is usually assumed in problems of image restoration from motion blur.[9,11] The blur identification here is based on the concept that the field correlation characteristics (spatial frequencies) along the direction of motion are affected mostly by the blur and are different from the characteristics in other directions. By high-pass filtering the blurred field, we can emphasize the PSF correlation prop-

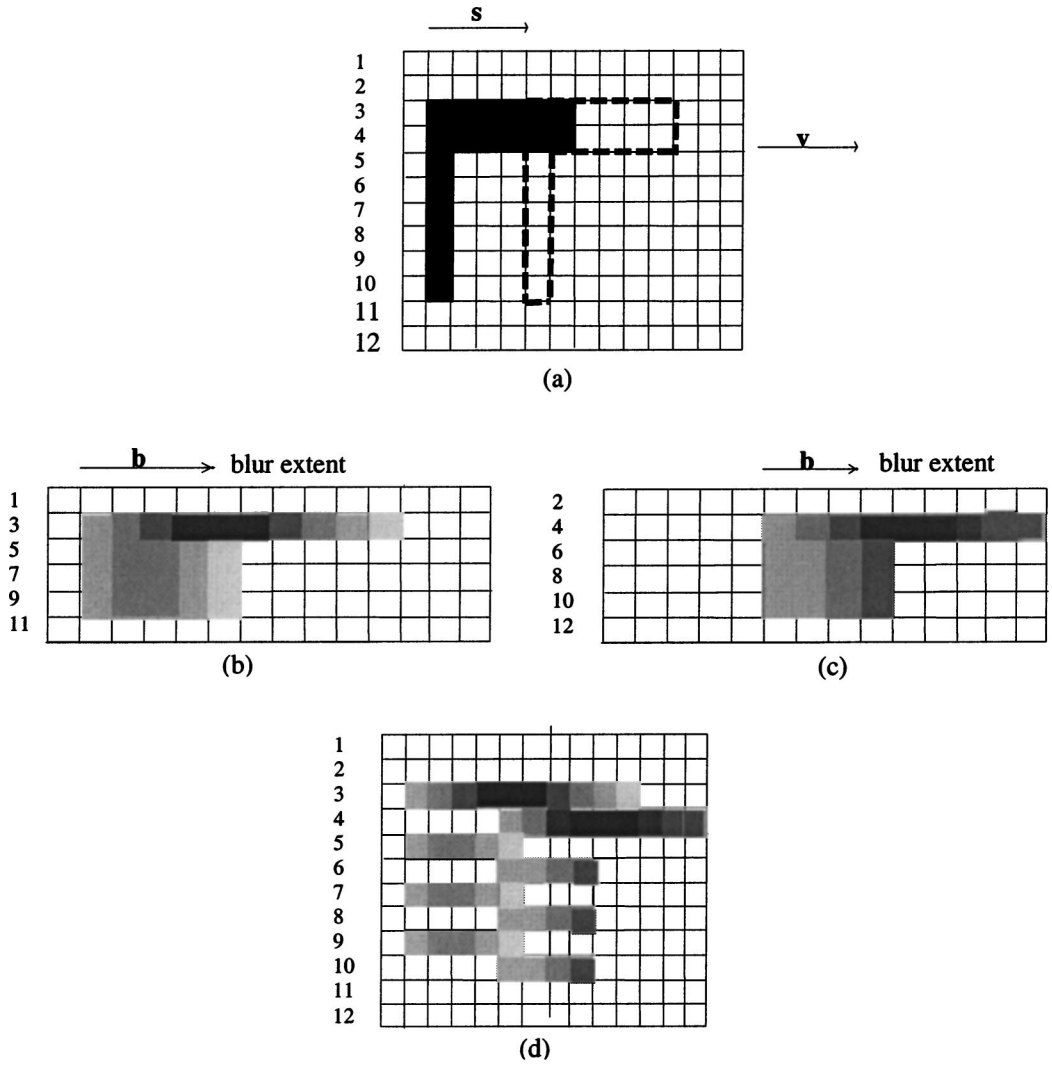

Fig. 1 An illustration of a variable velocity motion-distorted interlaced image formation. (a) The object locations at the beginning of the exposure instants in two successive fields. A horizontal motion is assumed, yielding a displacement vector length of $|\mathbf{s}|=4$ pixels. (b) The degraded odd field with $|\mathbf{b}|=3$ pixels blur extent. (c) The degraded even field with $|\mathbf{b}|=4$ pixels blur extent. The different gray shades at each field indicate a different instantaneous velocity $v(t)$ at each field. (d) The distorted interlaced image that is the composition of the displaced and blurred odd and even fields shown in (b) and (c).

erties at the expense of those of the original field.[13] For this purpose, a pseudo whitening filter is implemented in the motion direction and perpendicular to it. A simple high-pass filter can be used for this purpose. The motion direction required for PSF identification can be identified according to a method described in Ref. 8, assuming that the statistical properties of the field are approximately isotropic. Otherwise, the motion direction can be estimated according to the DV characteristics estimated by the block-matching algorithm (BMA), assuming that the motion direction does not change during the acquisition of both fields.

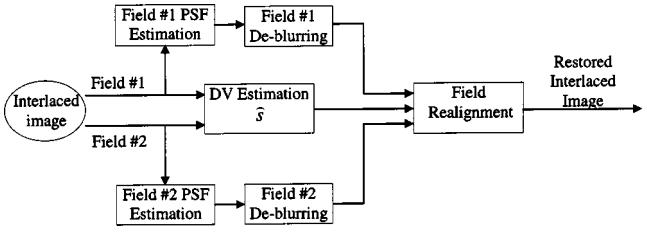

Fig. 2 Algorithm scheme for restoration of an interlaced image degraded by variable velocity motion.

After estimating the motion direction, a high-pass (whitening) filter is implemented in the motion direction and perpendicular to it. Implementation of such a filter forms patterns similar to the high-pass filtered PSF, surrounded by extremely suppressed decorrelated regions. The filtered field in the Fourier domain $\Delta G(u,v)$ can then be formulated as:

$$\Delta G(u,v)=G(u,v)W(v)W(u), \tag{1}$$

where u and v are the spatial frequency coordinates, and $W(v)$ and $W(u)$ are the high-pass filters perpendicular to and in the motion direction.

These patterns can be evaluated by performing an autocorrelation operation to all the filtered field lines in the motion direction, and then averaging them. Such operation suppresses the noise stimulated by the whitening operations, and causes cancellation of correlation properties left over from the field itself that can be different from one line to another. For many motion blur cases, the blur extent is the distance between the center of the average autocorrelation and its global minimum.[8]

Since the average autocorrelation function is usually similar to the autocorrelation of the filtered PSF,[8,13] the discrete Fourier transform of the average autocorrelation $S_{\Delta G}$ is also similar to the power spectrum of the filtered PSF $S_{\Delta \mathrm{PSF}}$, where $S_{\Delta \mathrm{PSF}}(u)=|H(u)\cdot W(u)|^2$ and $H(u)$ is the Fourier transform of the PSF, which is actually the optical transfer function (OTF) of the motion blurring system.[2] The modulation transfer function (MTF) of the blur is the absolute value of the OTF, and can be approximated by

$$\mathrm{MTF}(u)\approx\frac{[\overline{S}_{\Delta G}(u)]^{1/2}}{|W(u)|}. \tag{2}$$

The phase transfer function (PTF) can be computed from the MTF by[15]:

$$\mathrm{PTF}(u)=-\frac{1}{2\pi}\int_0^{2\pi}\ln\{\mathrm{MTF}(\alpha)\}\cot\frac{u-\alpha}{2}d\alpha. \tag{3}$$

The OTF used to restore the blurred image is:

$$H=\mathrm{MTF}\exp(j\,\mathrm{PTF}). \tag{4}$$

The identified PSF can then be obtained by inverse Fourier transforming the identified OTF.

3.2 *Estimation of the DV Using the Block-Matching Algorithm*

As a result of the motion between the exposures of the two image fields, object points in one field are shifted with respect to the adjacent object points in the other field. The DV specifies the distance and the direction of the displacement between two contiguous fields.

Many motion estimation approaches and methods have been developed, each optimal for certain situations and constrains.[16] The most common motion estimators are block-matching estimators.[17,18] Block-matching estimators have low sensitivity to noise, and they are suitable for parallel processing. Block-matching algorithms in general subdivide the image into a set of nonoverlapping areas (usually squares), and a single vector is calculated to give the best match between the block under consideration and those shifted in the previous image. The identified vector has a certain size and direction in the image plane and can be written as $\mathbf{s}=(s_x,s_y)^t$, where the size is

$$|\mathbf{s}|=(s_x^2+s_y^2)^{1/2}$$

and the direction is $\prec\mathbf{s}=\tan^{-1}(s_y/s_x)$. To reduce the computation load, only a limited search area is considered. The best match is carried out minimizing a suitable objective function. Various versions of the method exist for improving the computation load and speeding up the search time. Here we assume that the translational motion of the scene is limited to an extent D. A single square block from the center of the first field is chosen, and a search of a block of the same size in the second field that gives the minimum error in a mean square error (MSE) sense is performed. The block is taken from the middle of the field to permit a wide search in all directions. The size of the block area is variable according to the content of the image. For images containing many high-contrast random edges, a small block is sufficient to estimate precisely the global displacement vector. The autocorrelation function of even small blocks (e.g., 16×8 pixels) of images containing many high-contrast random edges is narrow and yields a precise MSE estimation. On the other hand, homogeneous and noisy images require larger blocks (e.g., 50×25 pixels). Since the field of view of the two fields is not similar [Fig. 1(b) versus Fig. 1(c)], objects at the boundary of one field may not appear in the other. This fact limits the block size. If the field size is $n\times m$, the block size is limited to $(n-2D)\times(m-2D)$, since the same blocks from different fields, which contain different information at the boundaries less distant than D pixels from all the edges, cannot be reliably matched.

3.3 *Image Restoration*

According to the restoration scheme presented in Fig. 2, an image restoration can be carried out after the estimation of the DV and blur functions. The blur estimation procedure presented in Sec. 3.1 is performed to each field, yielding a blur function for each field. Each estimated OTF from a field is then used to deblur the field using the Wiener filter.[19] The deblurred field $\hat{f}(m,n)$ will be:

$$\begin{aligned}\hat{f}(m,n)&=F^{-1}\{G(u,v)H_{\mathrm{Wiener}}(u,v)\}\\&=F^{-1}\left\{G(u,v)\frac{H^*(u,v)}{|H(u,v)|^2+\gamma}\right\},\end{aligned} \tag{5}$$

where $F^{-1}(\cdot)$ is the inverse Fourier transform, and γ is the relation between the spectra of the noise and the original unblurred field. Usually this relation is not known and γ is assumed to be a constant proportional to the inverse of the SNR.

Once the displacement vector $\mathbf{s}=(s_x,s_y)^t$ has been estimated, the realignment of the shifted fields is carried out by simply shifting the second field of vector $-\mathbf{s}$. Since the motion changes the field of view of the two fields, the effective realigned interlaced image is reduced to $(n-s_y)\times(m-s_x)$.

4 Results

Implementation results are presented here for both simulated (Sec. 4.1) and real-degraded (Sec. 4.2) interlaced images.

4.1 *Results for Synthetic Distortion*

In the first two examples, the effects of motion on interlaced images are simulated, and implementations of the image restoration procedures presented in Sec. 3 are per-

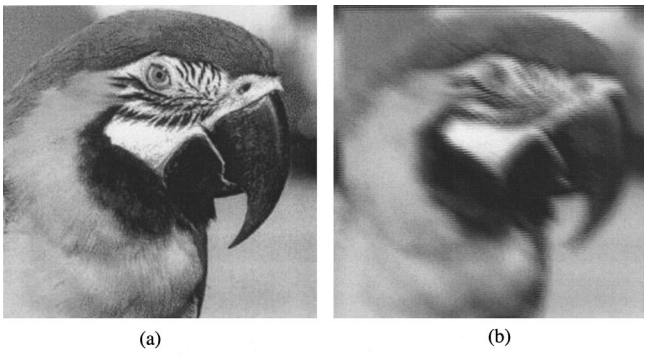

Fig. 3 (a) An original Parrot image. (b) The degraded interlaced image with blur and field displacement resulted from motion during and between successive exposures. The degradation is by accelerated motion function with $R=10$ in a direction of 20 deg. The blur size is 10 pixels in the odd field and 15 pixels in the even field, and the field displacement is 4 pixels.

formed. The odd and the even fields of the original unblurred Parrot image shown in Fig. 3(a) were shifted one with respect to the other in a direction of 20 deg and 4 pixels distance. Furthermore, each of the fields was blurred with a different accelerated motion function according to the convolution model. The PSF of accelerated motion is[2,7]:

$$\mathrm{PSF}(x)=\frac{1}{t_e(v_o^2+2ax)^{1/2}}, \tag{6}$$

where a is the acceleration, v_o is the initial velocity, and t_e is the exposure time. The accelerated motion parameter

$$R=v_o^2/a \tag{7}$$

describes the smoothness of the motion during the exposure. The odd field was blurred by an accelerated motion with $R=10$ in a direction of 20 deg and a blur extent of 10 pixels. The even field was blurred by the same function but with 15-pixel blur extent. The distorted image affected by both blur and displacement is presented in Fig. 3(b). Figure 4 shows a comparison between the PSFs used to blur the fields, and the PSFs estimated from the fields according to

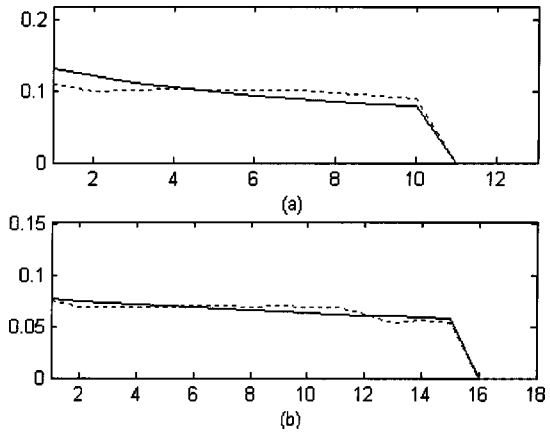

Fig. 4 True PSF (solid line) versus estimated PSF (dotted line) for the (a) odd and (b) even fields for the image of Fig. 3(b).

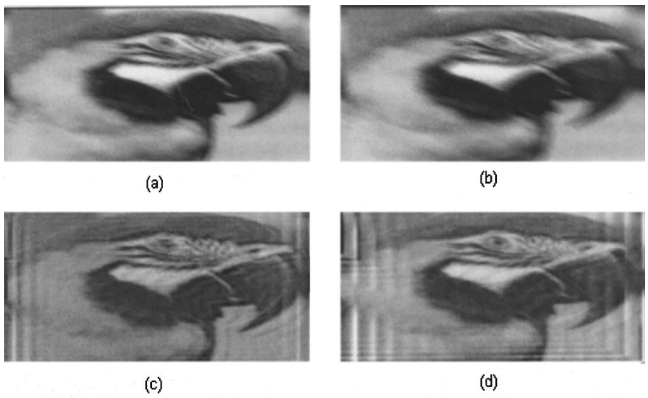

Fig. 5 (a) and (b) are the blurred odd and even fields of the distorted image shown in Fig. 3(b); (c) and (d) are the deblurred fields.

the procedure presented in Sec. 3.1. In Fig. 5 the blurred fields are compared to the deblurred fields using a Wiener filter [Eq. (5)] with their estimated OTFs. Periodical shadows of the edges with the extent of the PSF that appear in the deblurred image result from the nonperfect PSF estimates used with the Wiener restoration filter [Eq. (5)] The restored image presented in Fig. 6 is constructed by realigning the deblurred fields according to the correctly estimated DV.

The second example shows a case of interlaced image degradation due to the common problem of sinusoidal vibrations. In this case the motion function is periodic with an approximated form of a sine wave. This problem exists, for example, in imaging systems affected by circular motion, such as that of an engine. It is common in airborne or vehicular imaging systems. The vibration period can be shorter or longer than the field recording exposure. When the vibration period is longer, the problem is more complicated, since many different motion functions can occur, depending on the portion within the sine wave when the exposure took place.[2] In the example presented here, the odd and even fields were degraded by different portions of a sine wave, in a direction of 0 deg. The sine wave's amplitude was 40 pixels and its exposure duration was $0.1T$,

Fig. 6 The restored (deblurred and realigned) Parrot image.

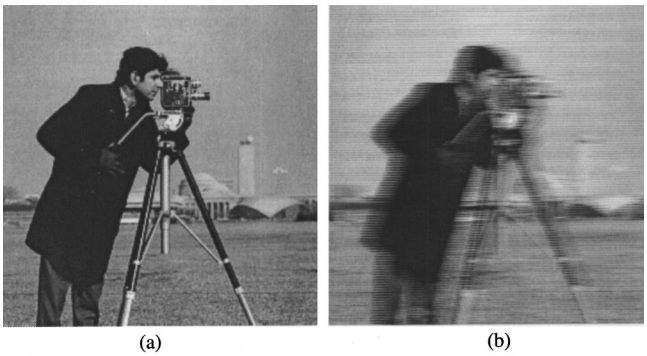

Fig. 7 (a) An original Cameraman image. (b) The degraded interlaced image, with blur and field displacement resulting from sinusoidal motion during and between the successive exposures, in a direction of 0 deg. The blur size is 8 pixels in the odd field and 19 pixels in the even field, and the field displacement is 5 pixels.

where T is the vibration period. The odd field was blurred by a portion of the sine starting from $T/4$. The time lag between the end of the exposure of the first field and the beginning of the exposure of the next field was $0.05T$. In this setup the blur extent of the odd field is 8 pixels and the blur extent of the even field is 19 pixels. Figure 7(b) shows the degraded version of Fig. 7(a), including the displaced blurred fields. A comparison between the PSFs used to blur the fields and the PSFs estimated from the fields is shown in Fig. 8. In Fig. 9 the blurred fields are compared to the deblurred fields using a Wiener filter with the estimated PSFs. The restored image presented in Fig. 10 is constructed from the deblurred fields realigned according to the estimated DV. In this case, the deblurred odd field may appear better than both fields realigned, in spite of the decreased vertical resolution, as the field contains half of the image lines.

4.2 *Results for Real Distorted Interlaced Images*

Figure 11 presents an interlaced image acquired by a high-resolution thermal imaging system (3- to 5-μm wavelength) manufactured by Controp Limited (Hod Hasharon, Israel). The interlaced image of neighborhood buildings (located about 1 to 2 km from the camera) was acquired

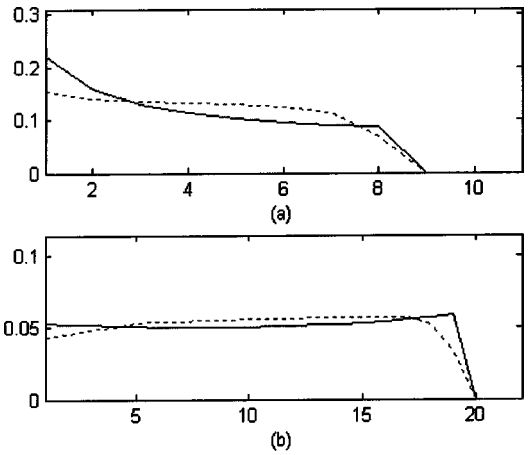

Fig. 8 Same as Fig. 4, but for the image of Fig. 7(b).

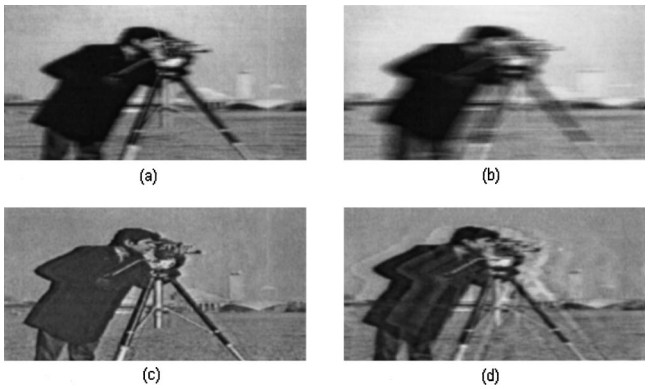

Fig. 9 Same as Fig. 5, but for the image of Fig. 7(b).

during a manual movement of the camera, and therefore is degraded by both blur and staircase effects as a result of the motion. Because the image was taken on a clear day, the atmospheric degradation in such distances was not significant. The blurred odd and even fields of the distorted image are shown in Figs. 12(a) and 12(b), respectively. The deblurred fields are shown in Figs. 12(c) and 12(d), respectively. It can be seen that the details of the buildings are clearer in the deblurred fields. The identified displacement between the fields was two pixels horizontally and one pixel vertically. The restored image (realigned deblurred fields) is shown in Fig. 13.

4.3 *Evaluation of the Results*

Image deblurring results are usually evaluated subjectively by the viewers. The reason for that is that human viewing is frequently the purpose of deblurring, and mathematical measures do not necessarily give reliable evaluation of the image quality as seen by the human observer. However, since motion during exposure blurs the image, it suppresses mainly the high-frequency content of the image (narrows its spectral distribution). Since image deblurring is expected to widen the spectral distribution of the image, a sense of the image quality can be evaluated by quantifying

Fig. 10 The restored (deblurred and realigned) Cameraman image.

Fig. 11 An original degraded interlaced image acquired by a thermal camera during a manual movement of the camera.

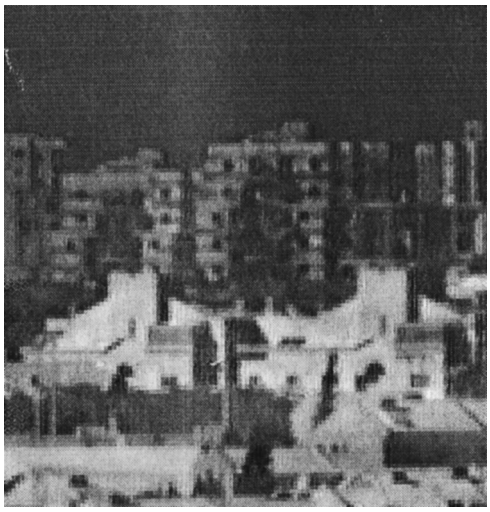

Fig. 13 The restored (deblurred and realigned) image.

the spectral content of the restored image with regard to the spectral contents of the blurred image and the original unblurred image (if it exists). To assess the spectral content of the image field, we calculated its radial spectrum:

$$S(r)=\int_0^{2\pi} S(r,\theta)\,d\theta,$$

where $S(r,\theta)$ is the PSD of the image field in polar coordinates,

$$r=(u^2+v^2)^{1/2}, \quad \theta=\tan^{-1}(v/u).$$

The normalized radial spectra for the original, blurred, and deblurred odd and even fields are presented in Figs. 14 and 15 for the Parrot and Cameraman images, respectively. For the real image case, the unblurred image does not exist, and we have the spectra of the recorded-blurred and deblurred fields shown in Fig. 16. It can be seen that the field spectrum is widened by the deblurring process. The higher quality of the original fields and the improvements in the deblurred fields appear in the mid-high frequencies, which are the frequencies mostly degraded by the motion. A single-number quantitative measure of the spectral content can be the area under the radial spectrum graph, $SA=\int S(r)dr$. A measure of the improvement in the spectral domain can be the proportion between the areas before and after deblurring. Defining by SAO, SAB, and SADB the areas under the radial spectra graphs of the original, blurred, and deblurred fields, respectively, SAO/SAB represents a comparative image quality measure (CIQM) of the original field versus the blurred field, and SADB/SAB represents a CIQM of the deblurred field versus the blurred field. Unlike the common MSE measure, this CIQM has the ability to indicate if an improvement is achieved (CIQM larger than one) or a degradation (CIQM smaller than one). Another advantage of this measure is that the original unblurred image is not required to asses the improvement of the deblurred image over the blurred one. This is important because frequently (as in the example in Sec. 4.2), the unblurred image does not exist. Table 1 presents the CIQMs for the examples shown in Figs. 3–12. It can be seen that all the results are above one, and there is a correlation between the values of the CIQMs presented in the table and the relative qualities of the images seen by the eye.

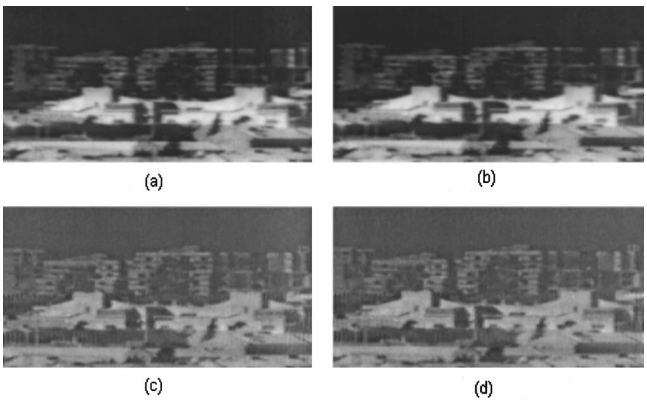

Fig. 12 Same as Fig. 5, but for the real-degraded interlaced image shown in Fig. 11.

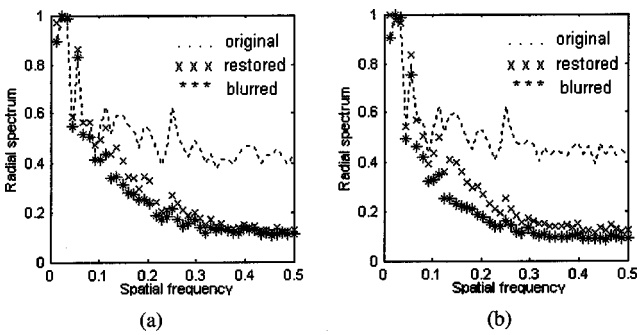

Fig. 14 Radial spectra of the original, blurred, and deblurred fields for the Parrot image. It can be seen that the image improvement appears in the mid-high frequencies, which are the frequencies mostly degraded by the motion.

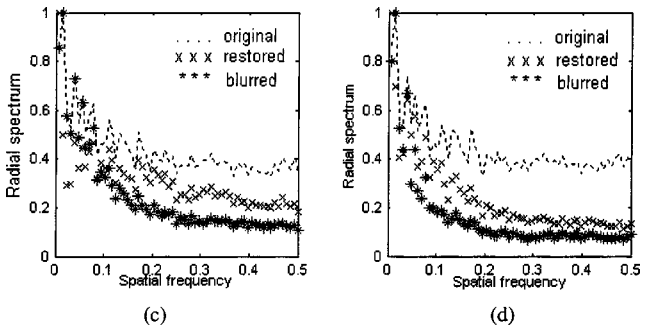

Fig. 15 Same as Fig. 14 but for the Cameraman image.

5 Summary and Conclusions

We deal with the problem of restoration of motion degraded interlaced images, which are the output of widely used imaging systems. The main novelty here is the consideration of variable velocity relative motion between the scene and the interlaced-type imaging system. This consideration is very important because in practice, a uniform velocity motion during exposure may not occur in many cases. In the case of an interlaced image degraded by a variable velocity motion, the blur within each field cannot be calculated from the DV (as performed in Ref. 12 for a uniform velocity motion), and it should be separately identified from the blurred fields themselves. For this purpose, a new motion blur identification technique recently developed[13] was applied. Other techniques for blind image restoration (where the degrading function is not *a priori* known) usually deal with uniform velocity motion or with cases where the degradation function can be determined by few (usually one or two) parameters.[9,11] In such cases correct identification of the parameters can lead to an almost perfect image restoration in simulations. The restoration algorithm presented in Sec. 3 considers estimation of the DV, estimation of the blur in each field, and restoration of the image using these estimates. Restoration results that depend on the accuracy of these estimates are presented for simulated and real-degraded images, and a spectral analysis of the results is performed. When the estimates of the PSFs are not perfect, restoration artifacts appear in the deblurred image as a result of a nonaccurate resulting restoration filter [Eq. (5)]. In some cases, especially such as vibration motion, one of the fields can be significantly less blurred than the other, depending on the random portion within the sine wave in which the exposures took place.

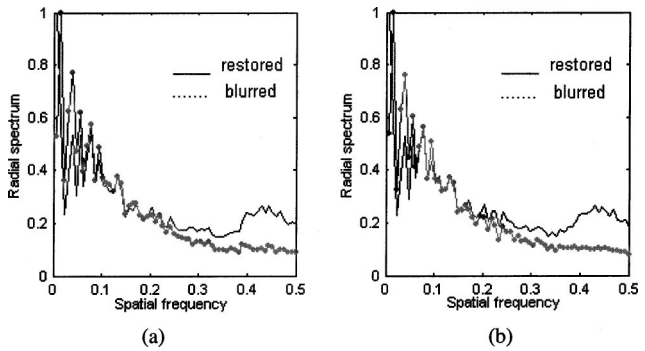

Fig. 16 Radial spectra of the recorded (blurred) and deblurred fields for the real-degraded IR image.

Table 1 The CIQMs that compare the spectral contents of the fields for the three examples presented in Figs. 3–12.

Image	Field	SAO/SAB	SADB/SAB
Parrot	Odd	1.88	1.03
	Even	2.18	1.16
Cameraman	Odd	1.80	1.24
	Even	2.69	1.47
Real IR image	Odd	⋯	1.12
	Even	⋯	1.16

Acknowledgments

The authors appreciate the fellowship support of the Ministry of Science and Technology, Jerusalem, and the support from the Paul Ivanier Center for Robotics and Production Management.

References

1. W. K. Pratt, *Digital Image Processing*, Wiley and Sons, New York (1978).
2. N. S. Kopeika, *A System Engineering Approach to Imaging*, Chap. 14, pp. 411–440, SPIE Optical Engineering Press, Bellingham, WA (1998).
3. B. Girod, ''Motion compensation: visual aspects, accuracy, and fundamental limits,'' in *Motion Analysis and Image Sequence Processing*, M. I. Sezan and R. L. Lagendijk, Eds., Chap. 5, pp. 135–139, Kluwer Academic, Boston (1993).
4. R. A. F. Belfor, R. L. Lagendijk, and J. Biemond, ''Subsampling of digital image sequences using motion information,'' in *Motion Analysis and Image Sequence Processing*, M. I. Sezan and R. L. Lagendijk, Eds., Chap. 9, Kluwer Academic, Boston (1993).
5. V. Markandey, T. Clatanoff, R. Gove, and K. Ohara, ''Motion adaptive deinterlacer for DMD (digital micromirror device) based digital television,'' *IEEE Trans. Consum. Electron.* **40**(3), 735–741 (1994).
6. R. Manduchi and G. M. Cortelazzo, ''Spectral characteristics and motion-compensated restoration of composite frames,'' *IEEE Trans. Image Process.* **4**(1), 95–99 (1995).
7. S. C. Som, ''Analysis of the effect of linear smear on photographic images,'' *J. Opt. Soc. Am. A* **61**(7), 859–864 (1971).
8. Y. Yitzhaky and N. S. Kopeika, ''Identification of blur parameters from motion blurred images,'' *CVGIP: Graph. Models Image Process.* **59**(5), 321–332 (1997).
9. M. Cannon, ''Blind deconvolution of spatially invariant image blurs with phase,'' *IEEE Trans. Acoust., Speech, Signal Process.* **Assp-24**(1), (1976).
10. *Digital Image Restoration*, A. K. Katsaggelos, Ed., Springer-Verlag, Berlin (1991).
11. G. Pavlovic and A. M. Tekalp, ''Maximum likelihood parametric blur identification based on a continuous spatial domain model,'' *IEEE Trans. Image Process.* **1**(4), 496–504 (1992).
12. A. Stern and N. S. Kopeika, ''Motion-distorted composite-frame restoration,'' *Appl. Opt.* **38**(5), 757–765 (1999).
13. Y. Yitzhaky, I. Mor, A. Lantzman, and N. S. Kopeika, ''A direct method for restoration of motion blurred images,'' *J. Opt. Soc. Am. A* **15**(6), 1512–1519 (1998).
14. Y. Yitzhaky, R. Milberg, S. Yohayev, and N. S. Kopeika, ''Comparison of direct blind deconvolution methods for motion-blurred images,'' *Appl. Opt.* **38**(20), 4325–4332 (1999).
15. B. Gold and C. M. Rader, *Digital Processing of Signals*, McGraw-Hill, Inc., New York (1969).
16. C. Stiller and J. Konrad, ''Estimating motion in image sequences—A tutorial on modeling and computation of 2D motion,'' *IEEE Trans. Signal Process.* **16**(4), 70–91 (1999).
17. T. Reuter, ''Standards conversion using motion compensation,'' *Signal Process.* **16**(1), 73–82 (1989).
18. S. Tubaro and F. Rocca, ''Motion field estimators and their application to image interpolation,'' in *Motion Analysis and Image Sequence Processing*, M. I. Sezan and R. L. Lagendijk, Eds., Chap. 6, pp. 160–165, Kluwer Academic, Boston (1993).
19. A. K. Jain, *Fundamentals of Digital Image Processing*, Prantice Hall, Englewood Cliffs, NJ (1989).

Yitzhak Yitzhaky received his BS, MS, and PhD degrees in electrical and computer engineering from Ben Gurion University, Israel, in 1993, 1995, and 2000, respectively. From 2000 to 2002 he was a postdoctoral research fellow at the Schepens Eye Research Institute, an affiliate of Harvard Medical School, Boston. Currently he is with the Electro-Optics Unit at Ben Gurion University, Israel. His research areas are mainly in the fields of image restoration, image enhancement, feature extraction, and vision.

Adrian Stern received his BSc, MSc, and PhD degrees from Ben-Gurion University of the Negev, Israel, in 1988, 1997, and 2003, respectively, all in electrical and computer engineering. He is now a postdoctoral fellow in the electrical and computer engineering department at University of Connecticut. His current research interests include 3-D imaging, optical encryption, sequences of images processing, image restoration, image and video compression, and imaging through atmosphere.